Integrative Biology

TECHNICAL INNOVATION

View Article Online
View Journal

Cite this: DOI: 10.1039/c5ib00054h

High-throughput screening for modulators of cellular contractile force†

Chan Young Park,[a] Enhua H. Zhou,[a] Dhananjay Tambe,[a] Bohao Chen,[b] Tera Lavoie,[b] Maria Dowell,[b] Anton Simeonov,[c] David J. Maloney,[c] Aleksandar Marinkovic,[a] Daniel J. Tschumperlin,[a] Stephanie Burger,[a] Matthew Frykenberg,[a] James P. Butler,[a] W. Daniel Stamer,[d] Mark Johnson,[e] Julian Solway,[b] Jeffrey J. Fredberg[a] and Ramaswamy Krishnan*[f]

Received 19th February 2015,
Accepted 1st May 2015

DOI: 10.1039/c5ib00054h

www.rsc.org/ibiology

When cellular contractile forces are central to pathophysiology, these forces comprise a logical target of therapy. Nevertheless, existing high-throughput screens are limited to upstream signalling intermediates with poorly defined relationships to such a physiological endpoint. Using cellular force as the target, here we report a new screening technology and demonstrate its applications using human airway smooth muscle cells in the context of asthma and Schlemm's canal endothelial cells in the context of glaucoma. This approach identified several drug candidates for both asthma and glaucoma. We attained rates of 1000 compounds per screening day, thus establishing a force-based cellular platform for high-throughput drug discovery.

Insight, innovation, integration

In high-throughput drug discovery that is targeted at contractile tissues, available drug screening technologies use varied biochemical or structural surrogates for contractile force rather than contractile force itself. As such, some hits are false while other potential hits could be missed. To fill this gap, we developed a new high-throughput method called contractile force screening (CFS) that utilizes cellular contractile force directly as a reporter, and establish feasibility in the context of asthma and glaucoma. CFS is likely to be a game-changer in drug discovery where a disease impacts cellular contractile force such as in the cases of vascular and cardiac disease, pulmonary arterial hypertension, asthma, glaucoma, and metastatic and invasive disease.

Introduction

In many organs and tissues, cellular contractile forces play a central role in physiology and pathophysiology. As such, modulation of cellular contractile forces is often the main therapeutic strategy. Commonplace examples are cardiac inotropes for cardiomyocytes,[1] bronchodilators for airway smooth muscle cells,[2] vasodilators for vascular smooth muscle cells,[3] and relaxants for skeletal muscle cells.[4] Cellular contractile forces are also important in metastasis and cancer cell invasion.[5,6] In each of these instances there clearly exist urgent unmet therapeutic needs.[7–9] Nevertheless, it has not previously been practical to use measurements of cellular contractile forces themselves as a primary read-out in high-throughput drug discovery. Instead, currently available high-throughput screening technologies have been limited to measurements of surrogates for contraction itself, including upstream effectors such as intracellular messengers, binding affinity assays against specific cell surface receptors or other moieties, protein expression and protein relocation, or morphological changes.[10–13]

The strength of these existing high-throughput approaches is that they are remarkably fast, but the weakness is that they stop short of incorporating and directly evaluating the main therapeutic target–cellular contractile force. Depending upon the assay, therefore, not only are certain drug candidates potentially missed, but also many of the corresponding hits might be found subsequently to have little or no impact on contractile force. Necessarily, efficacy and validation of these hits can only be established independently using old-fashioned

[a] Molecular and Integrative Physiological Sciences, Harvard School of Public Health, 665 Huntington Avenue, Boston, MA 02115, USA
[b] Departments of Medicine, University of Chicago, 5841 S. Maryland Avenue, Chicago, IL 60637, USA
[c] National Center for Advancing Translational Sciences, National Institutes of Health, 6701 Democracy Boulevard, Bethesda, MD 20892, USA
[d] Duke Eye Center, Duke University, 2351 Erwin Road, Durham, NC 27710, USA
[e] Department of Biomedical Engineering, Northwestern University, 2145 Sheridan Road, Evanston, IL 60208, USA
[f] Department of Emergency Medicine, Beth Israel Deaconess Medical Center, 99 Brookline Avenue, Boston, MA 02215, USA. E-mail: rkrishn2@bidmc.harvard.edu

† Electronic supplementary information (ESI) available: Details of any supplementary information available should be included here. See DOI: 10.1039/c5ib00054h

low throughput methods such as contractility measured in the isolated muscle strip[14] or reactivity measured in the living organism.[15] Cellular deformability has been proposed as a high-throughput basis for cell screening in the context of cancer,[16] malaria[17] and malignant pleural effusions[18] but these assays are limited to floating cells and are insensitive to depolymerization of actin, inhibition of myosin,[19] or modulation of adhesion proteins. In anchorage-dependent cells, and especially when contractile force is of concern, such assays are inapplicable. In the context of physiological and organ systems modeling, *in vitro* tissue constructs and organ-on-chip technologies are also promising[20–22] but, compared to the approach described below, are considerably more complex and thus less well suited for high levels of screening throughput. Overall, many potential drugs have been found *via* current high-throughput assays, but the majority of new molecular entities approved by US food and drug administration (FDA) continue to be discovered *via* traditional phenotypic assays.[23] Moreover, because 50% of drug candidates currently fail in phase II clinical trials,[24] it has been suggested that decreased failure rates and reduced development costs might be attained if disease-relevant endpoints were brought into drug discovery at an earlier stage.[25] To fill this gap, we describe here a new technology, contractile force screening (CFS), based upon straightforward measurement of cellular contractile force itself, which serves as the targeted physiological endpoint.

Materials and methods

Cell culture

Primary human airway smooth muscle (HASM) cells from 5 donors were obtained from lungs unsuitable for transplantation, as previously described.[26,27] Screening and secondary validations of both the Prestwick® and Chembridge DIVERSet® libraries were restricted to passage 7 cells from one donor. 10,000 cells per well were seeded onto assay plates in a medium containing 10% fetal bovine serum (FBS). After 2 hours of incubation, the serum containing medium was replaced with serum free medium containing insulin (5.7 μg mL^{-1}) and transferrin (5 μg mL^{-1}) instead of FBS for an additional 48 hours prior to experimentation.

Human endothelial cells of the inner wall of Schlemm's canal (SC) were obtained from post-mortem human eyes provided by Midwest Eye Bank, NDRI or Life Legacy as previously described;[28,29] passage 6–7 from 1 donor were used. Approximately 3200 to 6400 cells per well were seeded onto assay plates in a medium containing 1% FBS. Cells were grown in this medium for 2 days and in serum free medium supplemented with insulin-transferrin-selenium for an additional 12 hours prior to experimentation.

Preparation of drug mixtures

From the Prestwick Chemical Library®, we screened 1120 drugs. 4 drugs within the same column of the source plate were mixed together and distributed within drug plates as shown in Fig. S2 (ESI†). From the Chembridge DIVERSet Library®, we screened 10 000 compounds. 8 drugs within same column in the source plates were mixed together and distributed within drug plates as shown in Fig. S2 (ESI†).

Preparation of deformable substrates in 96-well plates

Polyacrylamide based gel substrates were miniaturized (schematic in Fig. S7, ESI†) in glass bottom 96-well plates using one of two methodologies. In the first method, each 96-well plate was treated with NaOH (6 N in water) for 1 h followed by silane solution ((3-aminopropyl)trimethoxysilane, 10% in water) for an additional 1 h. Next, red fluorescent bead solution (1 μm carboxylate-modified microspheres, Invitrogen, 2×10^{-4}% in water) was added to the wells and air-dried overnight. Dried glass surfaces were then treated with glutaraldehyde (0.25% in PBS) for 30 min and further washed and dried. Acrylamide gels (5.5% acrylamide, 0.076% bisacrylamide, Young's modulus = 1.8 kPa, thickness = 200 μm) were cast in each well using a custom-made gel caster[30] (Matrigen Life Technologies, CA). The gel surfaces were functionalized using sulfo-SANPAH (sulfosuccinimidyl-6-[4′-azido-2′-nitrophenylamino]hexanoate, 0.2 mg mL^{-1}), coated with green beads (0.2 μm sulfate microspheres, Invitrogen, 2×10^{-3}% in water),[31] coated with bovine collagen I (40 μg mL^{-1} in PBS)[27] and were stored at 4 °C (Fig. 1A).

In the second method, each 96-well plate was treated with silane (γ-methacryloxypropyltrimethoxysilane, 0.4% in water), and a first layer of acrylamide gel substrate (8% acrylamide, 0.1% bisacrylamide, and 0.4% acrylic acid *N*-hydroxysuccinimide ester (NHS),[32] Young's modulus ≈2.5 kPa, thickness ≈200 μm) was prepared using the custom-made gel caster described above. The casting procedure was repeated for a second layer of gel[33] with the same composition plus 2% vol/vol red beads (0.5 μm carboxylate-modified microspheres, Invitrogen); this top layer was prepared exceedingly thin to promote fluorescent bead dispersion within a single horizontal plane. The gels were coated with bovine collagen I (10 μg mL^{-1} in PBS) (Fig. S1, ESI†).

Measurements of contractile forces using Fourier-transform traction microscopy

The 96-well plate was mounted within a heated chamber (37 °C) upon a motorized stage and imaged using an inverted microscope (DMI 6000B, Leica Inc.). In each well, three images were obtained in quick succession: one phase contrast image of cells and a pair of fluorescent images of beads (Fig. 1A). The image set was obtained before plating cells (*reference*), immediately prior to adding drugs (*baseline*), and 1 h after drug addition (*treatment*). By comparing fluorescent images obtained during *baseline* or *treatment* with the corresponding image from *reference*, we computed the cell-exerted displacement field.[34,35] From the displacement field, we computed the contractile force (per unit area) using Fourier-transform traction microscopy[34,35] modified to the case of cell monolayers.[32,35–37] This modified approach takes into consideration effects of finite gel thickness as well as force imbalances associated with the microscope field of view as we described previously.[35,37] From each force map (Fig. 1B), we computed the root mean squared value to represent the averaged

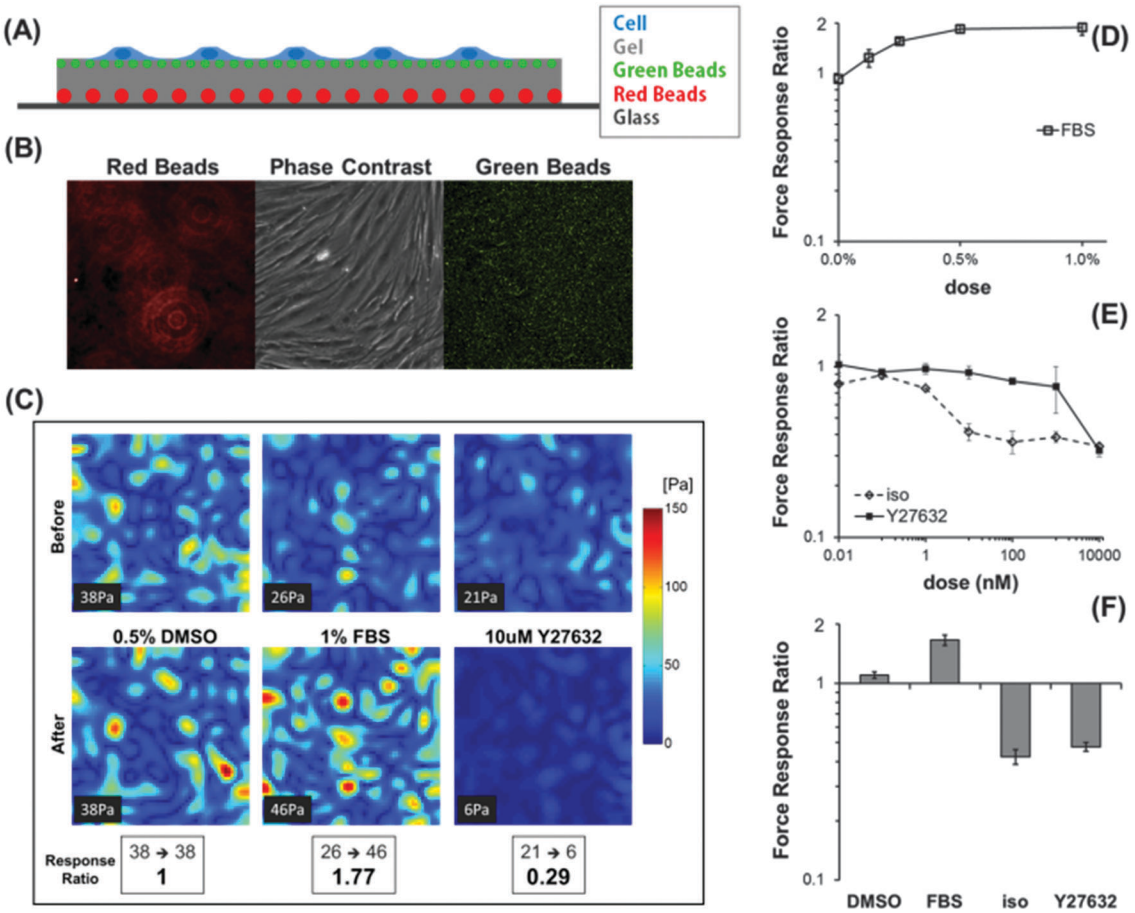

Fig. 1 Contractile force screening (CFS). (A) Acrylamide-based hydrogels were miniaturized in glass bottom 96-well plates. (B) In each well, three images were obtained in quick succession: one phase contrast image of cells and a pair of fluorescent images of beads. (C) Representative maps of cellular contractile force (per unit area) before (top) and 1 h after addition of drugs (bottom) together with the root mean square (RMS) tractions indicated in the lower-left corner. Drug effects were quantified as the force response ratio, namely, the RMS tractions before *versus* after drug addition. The dose-dependent force response ratios of (D–E) human airway smooth muscle (HASM) cells, and, (F) Schlemm's canal (SC) endothelial cells were measured using contractile agonist (FBS, fetal bovine serum) and relaxing agonists (iso, isoproterenol; Y27632, rho kinase inhibitor). Plotted in (D) and (E) are the average values ± SD (n = 4) and in (F) the average values ± SEM (n = 4).

contractile force. Throughout the paper, we use the generic word "force" to mean the traction, which is the contractile force (per unit area) that cells exert on their substrate.

Evaluation of CFS

A commonly used statistical parameter to evaluate accuracy and sensitivity of high-throughput assay is the Z'-factor.[38] Notably, assays with Z'-factor ≥ 0.5 are typically considered optimized for high throughput screening.[39] But Z' has limitations such as its oversensitivity to the data distribution or outliers.[40] Therefore, alternative metrics have been suggested including the robust Z'-factor.[41] The variability of cellular stiffness and contractile force in HASM cells are known to be high[42,43] and the distribution of the force response ratios are closer to a log-normal distribution (Fig. 2). Hence, we used here the robust Z'-factor as a quality metric of CFS. The robust Z'-factor is defined as:

$$\text{robust } Z' = 1 - \frac{3(\text{S1} + \text{S2})}{|\text{X1} - \text{X2}|}$$

where, S1 and S2 are the median absolute deviations of negative and positive controls and X1 and X2 are the medians of negative and positive controls. We used vehicle control (water, 0.01%) as the negative control and rho-kinase inhibitor, Y27632 (12 μM) as the positive control. The control compounds were distributed equally in the 96 well-plate and examined for their effects on cellular contractile forces. From these measurements, the computed robust Z'-factor was 0.605 (Fig. S3, ESI†).

Perfusion of mouse eyes

The subject of this report is CFS technology, not the hits themselves, which now become candidates of interest for future investigation. Nevertheless, to establish for CFS not only proof of principle but also potential utility, we selected one hit, alprostadil, for further validation at the organ level. Alprostadil was tested for its ability to increase outflow facility in enucleated mouse eyes. The mouse eyes were obtained from 11 C57BL/6 mice of either gender, aged 10 weeks to 7 months old at time of death. Enucleated eyes were stored in phosphate buffered saline

at 4 °C until perfusion, typically 1–3 hours. The perfusion method follows previously described techniques that we developed[44–48] with a few modifications. Briefly, each enucleated eye was affixed onto a post using cyanoacrylate glue; stabilizing the eye for cannulation of the anterior chamber. Eyes were cannulated with a 33-gauge beveled-tip needle (Nanofil; World Precision Instruments, Europe; Hitchin, UK) backfilled with 1 μM alprostadil or vehicle (ethanol, 1: 10 000). Housed in a humidified chamber, eyes were perfused in pairs and randomized for each perfusion as to whether drug or vehicle was perfused first. The needle was connected *via* pressure tubing to a glass syringe (25 μL; Hamilton GasTight, Reno, NV) that was mounted and controlled by motorized syringe pump (PHD Ultra; Harvard Apparatus, MA). Custom written LabVIEW software (National Instruments Corp., Austin, TX) served to monitor intraocular pressure (IOP) (*via* in line 142PC01G pressure transducer; Honeywell, Columbus, OH) and control the flow rates delivered by the syringe pump into the eye to maintain a user-defined IOP (13). Both experimental and control eyes were initially held at 8 mmHg for 45 minutes using a fluid reservoir to facilitate exposure of cells in the outflow pathway to drug (or vehicle). Subsequently, eyes were perfused at sequential pressure steps of 4, 8, 15 and 20 mmHg. Each pressure step was maintained for 20–30 minutes to obtain a minimum of 10 minutes of stable flow data, from which an average stable flow rate was calculated for each pressure step. Data from an individual eye was considered acceptable if a stable flow rate was achieved in at least 3 of the 4 pressure steps. Outflow facility was found following the general principle of the two-level constant pressure perfusion procedure introduced by Barany.[49] Here we measured flow rate (Q) at four pressures (P), and then found the outflow facility using a regression analysis by fitting the data to the following relationship using SPSS:

$$Q = a_0 + a_1 \cdot P + a_2 \cdot P \cdot \mathrm{DRUG}$$

where DRUG = 0 is the control case and DRUG = 1 when alprostadil was applied. a_1 is the outflow facility for control eyes and $a_1 + a_2$ that for eyes after alprostadil application.

Results and discussion

Contractile force screening (CFS) is based upon Fourier-transform traction microscopy,[34–37] which we adapted to 96-well plates.[30] In each well, polyacrylamide gel surfaces were labeled with fluorescent markers,[31] functionalized with collagen,[27] and covered with cells grown to near confluence[35–37,50] (Fig. 1A and B and Fig. S1, ESI†). Using an automated fluorescence microscope, we quantified in each well the average (*i.e.* root mean square) cellular contractile forces before and after adding drugs. Drug effects were quantified as the 'force response ratio', namely, the contractile force before *versus* after drug addition (Fig. 1C). For example, in a representative well, the average contractile force generated by cultured primary human airway smooth muscle (HASM) cells at baseline was 38 Pa (left column in Fig. 1C), and force did not change after adding vehicle alone (dimethyl sulfoxide (DMSO), 0.5%, final concentration); thus, the force response ratio for vehicle was close to 1. In other representative wells, the force response ratio for fetal bovine serum (FBS, 1%), which is known to increase contraction,[51] was 1.77 (middle column in Fig. 1C), while that for the rho kinase inhibitor Y27632 (10 μM),[52] known to impair contraction, was 0.29 (right column in Fig. 1C). Force response ratios revealed dose-dependent increases or decreases in cellular contractile force induced by FBS (Fig. 1D), Y27632, and the airway smooth muscle cell relaxant isoproterenol (Fig. 1E). Furthermore, using these force response ratios, CFS demonstrated that the robust Z'-factor was bigger than 0.6 (methods; Fig. S3, ESI†), thus confirming that the force response ratio provides a methodologically simple, physiologically relevant, and statistically valid index for identifying compounds that modulate cellular contractile forces.

To test the utility of CFS in the context of drug repurposing for use in asthma, we focused upon HASM cells. During an acute asthma attack, contractile forces generated by airway smooth muscle, cells act to constrict the airway and thus obstruct airflow. To dilate constricted airways, asthma patients use bronchodilators to reduce these contractile forces and thus allow the airway to open more fully, but currently available bronchodilator medications often fail to relax that muscle sufficiently, especially in severe asthma.[2] Therefore, we screened the Prestwick Chemical Library®, comprised of 1120 drugs already approved by the FDA or European Medicines Agency (EMA), to identify which among these might be an unanticipated candidate to relax airway smooth muscle cells in asthma. Each datum plotted in Fig. 2A (left panel) represents the average of quadruplicate measurements of a mixture of 4 drugs per well, with a concentration of 6.5 μM for each in the initial screen; the middle panel is the histogram of all responses and the right panel is the rank-ordered response. Mixtures that modulated contractile force appreciably – termed positives – were later retested individually to identify the active drugs – termed hits. Most mixtures did not change cellular contractile forces appreciably. Several mixtures increased the force response ratio more than did FBS, and, more importantly, several mixtures decreased the response ratio as much as or more than control relaxant compounds. From 280 mixtures tested, we selected 16 mixtures as positives (shown in red in Fig. 2A) that were found to blunt contractile force appreciably. After retesting drugs individually, we found 15 hits; 9 were β-adrenergic receptor agonists and 3 (alprostadil,[53,54] ethaverine hydrochloride[55] and kaempferol[56,57]) were already well-known as smooth muscle relaxants (Tables 1A and 2A, ESI†). However, the HASM relaxant effects of three drugs were unexpected: chicago sky blue, terconazole and levonordefrin (α-methylnorepinephrine). Although these unanticipated hits remain to be validated before they can repurposed as bronchodilator drugs, these findings confirm the ability of CFS to identify novel candidate relaxants of airway smooth muscle in the context of asthma.

To validate further the utility of CFS in a different disease context, we turned to human endothelial cells of Schlemm's

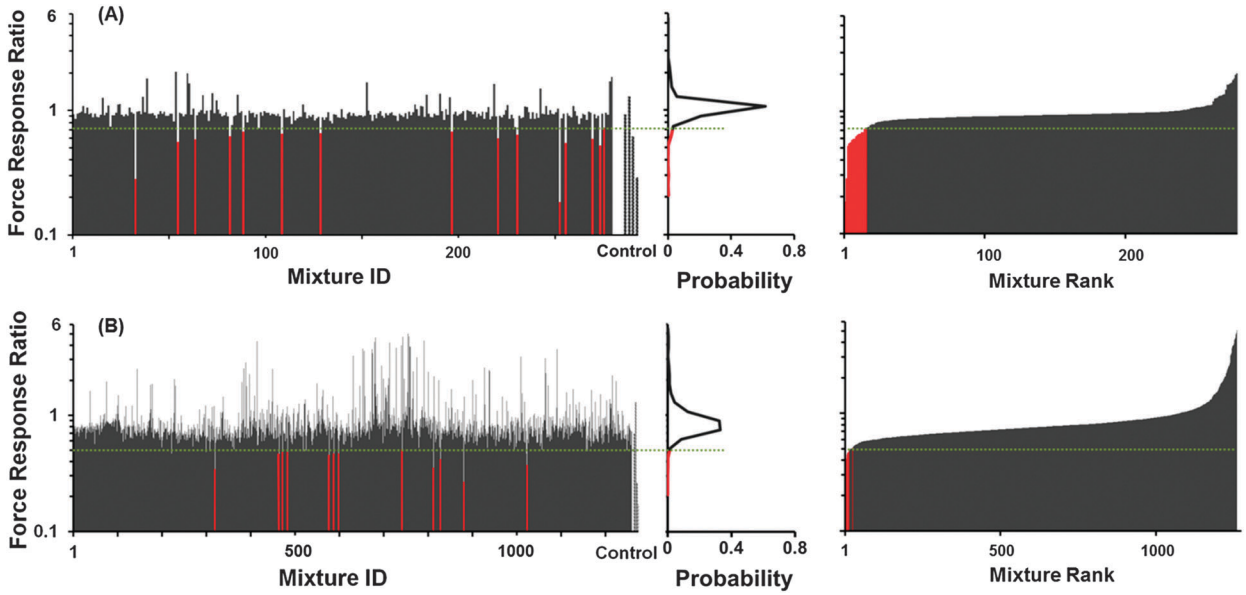

Fig. 2 CFS for novel bronchodilatory drugs. (A) Each datum corresponds to the force response ratio for each mixture from (A) the Prestwick® chemical library, or, (B) the Chembridge DIVERset® library. Using the green dotted line as a cut-off, we selected for further evaluation the mixtures with the greatest relaxant effect, shown as red vertical lines. Shown on the far right in the left panel are the response ratio for 4 controls; DMSO, FBS, isoproterenol, and Y27632. The middle panel is the histogram with corresponding cut-off line and the right panel is the rank-ordered response. A few mixtures in top ranks were disregarded based on variability within quadruplicate measurements.

canal (SC) in the context of drug repurposing for use in glaucoma, which remains a leading cause of blindness.[58] All current drug treatments and surgical treatments for glaucoma target reduction of intraocular pressure, but many patients remain refractory to those treatments. Because excessive contraction of the SC cell has been implicated recently in the etiology of glaucoma,[29,59] we first tested human SC cells using the control drugs described above and found that they modulated contractile force of SC cells much as they did in HASM cells (Fig. 1F). Next, from the Prestwick Chemical Library®, 17 individual drugs were identified as hits that blunted SC cell contraction. One was a toxin (Sanguinarine), 9 were β-adrenergic receptor agonists already well-known as SC relaxants, and one was a vasodilator (Alprostadil, Tables 1B and 2B, ESI†). Alprostadil was the most potent of these hits; further inspection revealed that alprostadil reduced contractile force of SC cells in a dose-dependent manner (Fig. S4A, ESI†). *Ex vivo* perfusion studies demonstrated that alprostadil lowers outflow resistance by 30%, thus confirming efficacy at the organ-level of a drug candidate identified by CFS (Fig. S4B, ESI†).

Having established the feasibility of using CFS in a small library like the Prestwick Chemical Library®, we turned next to larger libraries and questions of throughput. In a subset comprising 10 000 compounds selected randomly from the Chembridge DIVERset®, we set up each drug plate to contain 35 different compound mixtures and 5 controls, with each mixture consisting of 8 compounds. Since hits are few (Fig. 2), the probability of interactions between compounds or cancelling effects in any given well is small. For this screening, we used HASM cells to find novel candidate bronchodilators. With drug incubation time of 1 h and using a single microscope, we screened all 10 000 compounds at the rate of 1120 compounds per screening day (Fig. S5, ESI†). From this screen, we found 12 positives (Fig. 2B) and finally 2 hits that were closely related structurally. Further studies of these compounds revealed that contractile forces in HASM cells were reduced substantially, non-toxically, and in a dose-dependent manner (Fig. S6, ESI†).

Conclusions

In summary, contractile force screening is a high throughput technology that directly addresses the physiologic target of interest – contractile force – with an overall throughput on the order of at least a thousand compounds per microscope per day. Because this study did not employ automation or robotic handing, substantially higher levels of throughput should be readily attainable. CFS can thus fill an important methodological void in the middle ground between high-throughput but relatively non-physiological approaches on the one hand and physiological but low-throughput animal or tissue-based approaches on the other. As such, CFS has the potential to facilitate drug discovery and drug repurposing in any circumstance in which modulation of contractile force is the logical therapeutic target, including vascular and cardiac disease, pulmonary arterial hypertension, asthma, glaucoma, and metastatic and invasive disease.

Acknowledgements

The authors are grateful to Dr Reynold Panettieri at University of Pennsylvania for providing primary HASM cells, to the Institute for

Genomics and Systems Biology at University of Chicago for preparing the drug plates, and to the Institute of Chemistry and Cell Biology at Harvard Medical School for technical assistance. We gratefully acknowledge the critical comments of Emil Millet and Dr Ajit Jadhav and the support provided by the National Institutes of Health grants R01EY019696, R01HL102373, R01HL107561, P01HL120839, and UH2HL123816.

Notes and references

1 C. B. Overgaard and V. Dzavik, *Circulation*, 2008, **118**, 1047–1056.
2 P. J. Barnes, *Nat. Rev. Drug Discovery*, 2004, **3**, 831–844.
3 M. Humbert, O. Sitbon and G. Simonneau, *N. Engl. J. Med.*, 2004, **351**, 1425–1436.
4 S. See and R. Ginzburg, *Am. Fam. Physician*, 2008, **78**, 365–370.
5 E. Jonietz, *Nature*, 2012, **491**, S56–S57.
6 D. Wirtz, K. Konstantopoulos and P. C. Searson, *Nat. Rev. Cancer*, 2011, **11**, 512–522.
7 G. Hasenfuss and J. R. Teerlink, *Eur. Heart J.*, 2011, **32**, 1838–1845.
8 M. E. Wechsler, *Am. J. Med.*, 2014, **127**, 1049–1059.
9 A. Seferian and G. Simonneau, *Eur. Respir. Rev.*, 2013, **22**, 217–226.
10 F. Sams-Dodd, *Drug Discovery Today*, 2005, **10**, 139–147.
11 D. Brown, *Drug Discovery Today*, 2007, **12**, 1007–1012.
12 W. Zheng, N. Thorne and J. C. McKew, *Drug Discovery Today*, 2013, **18**, 1067–1073.
13 F. Zanella, J. B. Lorens and W. Link, *Trends Biotechnol.*, 2010, **28**, 237–245.
14 J. J. Fredberg, D. S. Inouye, S. M. Mijailovich and J. P. Butler, *Am. J. Respir. Crit. Care Med.*, 1999, **159**, 959–967.
15 A. M. Holmes, R. Solari and S. T. Holgate, *Drug Discovery Today*, 2011, **16**, 659–670.
16 J. Guck, S. Schinkinger, B. Lincoln, F. Wottawah, S. Ebert, M. Romeyke, D. Lenz, H. M. Erickson, R. Ananthakrishnan, D. Mitchell, J. Kas, S. Ulvick and C. Bilby, *Biophys. J.*, 2005, **88**, 3689–3698.
17 J. M. Mauritz, T. Tiffert, R. Seear, F. Lautenschlager, A. Esposito, V. L. Lew, J. Guck and C. F. Kaminski, *J. Biomed. Opt.*, 2010, **15**, 030517.
18 H. T. Tse, D. R. Gossett, Y. S. Moon, M. Masaeli, M. Sohsman, Y. Ying, K. Mislick, R. P. Adams, J. Rao and D. Di Carlo, *Sci. Transl. Med.*, 2013, **5**, 212ra163.
19 D. R. Gossett, H. T. Tse, S. A. Lee, Y. Ying, A. G. Lindgren, O. O. Yang, J. Rao, A. T. Clark and D. Di Carlo, *Proc. Natl. Acad. Sci. U. S. A.*, 2012, **109**, 7630–7635.
20 W. R. Legant, A. Pathak, M. T. Yang, V. S. Deshpande, R. M. McMeeking and C. S. Chen, *Proc. Natl. Acad. Sci. U. S. A.*, 2009, **106**, 10097–10102.
21 A. P. Nesmith, A. Agarwal, M. L. McCain and K. K. Parker, *Lab Chip*, 2014, **14**, 3925–3936.
22 D. Huh, B. D. Matthews, A. Mammoto, M. Montoya-Zavala, H. Y. Hsin and D. E. Ingber, *Science*, 2010, **328**, 1662–1668.
23 D. C. Swinney and J. Anthony, *Nat. Rev. Drug Discovery*, 2011, **10**, 507–519.
24 S. M. Paul, D. S. Mytelka, C. T. Dunwiddie, C. C. Persinger, B. H. Munos, S. R. Lindborg and A. L. Schacht, *Nat. Rev. Drug Discovery*, 2010, **9**, 203–214.
25 P. Lang, K. Yeow, A. Nichols and A. Scheer, *Nat. Rev. Drug Discovery*, 2006, **5**, 343–356.
26 R. A. Panettieri, Jr., *Methods Mol. Med.*, 2001, **56**, 155–160.
27 C. Y. Park, D. Tambe, A. M. Alencar, X. Trepat, E. H. Zhou, E. Millet, J. P. Butler and J. J. Fredberg, *Am. J. Physiol.: Cell Physiol.*, 2010, **298**, C1245–C1252.
28 W. D. Stamer, B. C. Roberts, D. N. Howell and D. L. Epstein, *Invest. Ophthalmol. Visual Sci.*, 1998, **39**, 1804–1812.
29 E. H. Zhou, R. Krishnan, W. D. Stamer, K. M. Perkumas, K. Rajendran, J. F. Nabhan, Q. Lu, J. J. Fredberg and M. Johnson, *J. R. Soc., Interface*, 2012, **9**, 1144–1155.
30 J. D. Mih, A. S. Sharif, F. Liu, A. Marinkovic, M. M. Symer and D. J. Tschumperlin, *PLoS One*, 2011, **6**, e19929.
31 A. Marinkovic, J. D. Mih, J. A. Park, F. Liu and D. J. Tschumperlin, *Am. J. Physiol.: Lung Cell. Mol. Physiol.*, 2012, **303**, L169–L180.
32 X. Serra-Picamal, V. Conte, R. Vincent, E. Anon, D. T. Tambe, E. Bazellieres, J. P. Butler, J. J. Fredberg and X. Trepat, *Nat. Phys.*, 2012, **8**, 628–634.
33 P. C. Bridgman, S. Dave, C. F. Asnes, A. N. Tullio and R. S. Adelstein, *J. Neurosci.*, 2001, **21**, 6159–6169.
34 J. P. Butler, I. M. Tolic-Norrelykke, B. Fabry and J. J. Fredberg, *Am. J. Physiol.: Cell Physiol.*, 2002, **282**, C595–C605.
35 X. Trepat, M. R. Wasserman, T. E. Angelini, E. Millet, D. A. Weitz, J. P. Butler and J. J. Fredberg, *Nat. Phys.*, 2009, **5**, 426–430.
36 J. H. Kim, X. Serra-Picamal, D. T. Tambe, E. H. Zhou, C. Y. Park, M. Sadati, J. A. Park, R. Krishnan, B. Gweon, E. Millet, J. P. Butler, X. Trepat and J. J. Fredberg, *Nat. Mater.*, 2013, **12**, 856–863.
37 D. T. Tambe, C. C. Hardin, T. E. Angelini, K. Rajendran, C. Y. Park, X. Serra-Picamal, E. H. Zhou, M. H. Zaman, J. P. Butler, D. A. Weitz, J. J. Fredberg and X. Trepat, *Nat. Mater.*, 2011, **10**, 469–475.
38 J. H. Zhang, T. D. Chung and K. R. Oldenburg, *J. Biomol. Screening*, 1999, **4**, 67–73.
39 W. F. An and N. Tolliday, *Mol. Biotechnol.*, 2010, **45**, 180–186.
40 A. Birmingham, L. M. Selfors, T. Forster, D. Wrobel, C. J. Kennedy, E. Shanks, J. Santoyo-Lopez, D. J. Dunican, A. Long, D. Kelleher, Q. Smith, R. L. Beijersbergen, P. Ghazal and C. E. Shamu, *Nat. Methods*, 2009, **6**, 569–575.
41 X. D. Zhang, *Genomics*, 2007, **89**, 552–561.
42 B. Fabry, G. N. Maksym, S. A. Shore, P. E. Moore, R. A. Panettieri, Jr., J. P. Butler and J. J. Fredberg, *J. Appl. Physiol.*, 2001, **91**, 986–994.
43 R. Krishnan, C. Y. Park, Y. C. Lin, J. Mead, R. T. Jaspers, X. Trepat, G. Lenormand, D. Tambe, A. V. Smolensky, A. H. Knoll, J. P. Butler and J. J. Fredberg, *PLoS One*, 2009, **4**, e5486.
44 Y. Lei, D. R. Overby, A. Boussommier-Calleja, W. D. Stamer and C. R. Ethier, *Invest. Ophthalmol. Visual Sci.*, 2011, **52**, 1865–1871.

45 A. Boussommier-Calleja, J. Bertrand, D. F. Woodward, C. R. Ethier, W. D. Stamer and D. R. Overby, *Invest. Ophthalmol. Visual Sci.*, 2012, **53**, 5838–5845.
46 A. Boussommier-Calleja and D. R. Overby, *Invest. Ophthalmol. Visual Sci.*, 2013, **54**, 8251–8258.
47 W. D. Stamer, Y. Lei, A. Boussommier-Calleja, D. R. Overby and C. R. Ethier, *Invest. Ophthalmol. Visual Sci.*, 2011, **52**, 9438–9444.
48 M. E. Rogers, I. D. Navarro, K. M. Perkumas, S. M. Niere, R. R. Allingham, C. E. Crosson and W. D. Stamer, *Invest. Ophthalmol. Visual Sci.*, 2013, **54**, 6655–6661.
49 E. H. Bárány, *Invest. Ophthalmol. Visual Sci.*, 1964, **3**, 135–143.
50 R. Krishnan, D. D. Klumpers, C. Y. Park, K. Rajendran, X. Trepat, J. van Bezu, V. W. van Hinsbergh, C. V. Carman, J. D. Brain, J. J. Fredberg, J. P. Butler and G. P. van Nieuw Amerongen, *Am. J. Physiol.: Cell Physiol.*, 2011, **300**, C146–C154.
51 N. A. Abdullah, M. Hirata, K. Matsumoto, H. Aizawa, R. Inoue, S. Hamano, S. Ikeda, Z. Xie, N. Hara and Y. Ito, *Am. J. Physiol.*, 1994, **266**, L528–L535.
52 M. Uehata, T. Ishizaki, H. Satoh, T. Ono, T. Kawahara, T. Morishita, H. Tamakawa, K. Yamagami, J. Inui, M. Maekawa and S. Narumiya, *Nature*, 1997, **389**, 990–994.
53 W. J. Sweatman and H. O. Collier, *Nature*, 1968, **217**, 69.
54 Z. Wajima, T. Shiga, T. Yoshikawa, A. Ogura, K. Imanaga, T. Inoue and R. Ogawa, *Anesth. Analg.*, 2003, **97**, 456–460, table of contents.
55 W. J. Oswald and D. H. Baeder, *South. Med. J.*, 1975, **68**, 1481–1484.
56 L. K. Leal, M. F. Costa, M. Pitombeira, V. M. Barroso, E. R. Silveira, K. M. Canuto and G. S. Viana, *Life Sci.*, 2006, **79**, 98–104.
57 E. A. Townsend and C. W. Emala, Sr., *Am. J. Physiol.: Lung Cell. Mol. Physiol.*, 2013, **305**, L396–L403.
58 M. Kahook, J. S. Schuman and D. L. Epstein, *Chandler and Grant's Glaucoma*, Slack Incorporated, 5th edn, 2013, ISBN: 1556429541.
59 D. R. Overby, E. H. Zhou, R. Vargas-Pinto, R. M. Pedrigi, R. Fuchshofer, S. T. Braakman, R. Gupta, K. M. Perkumas, J. M. Sherwood, A. Vahabikashi, Q. Dang, J. H. Kim, C. R. Ethier, W. D. Stamer, J. J. Fredberg and M. Johnson, *Proc. Natl. Acad. Sci. U. S. A.*, 2014, **111**, 13876–13881.